PHYSICAL REVIEW A, VOLUME 64, 011401(R)

Realization of bichromatic optical superlattices

A. Görlitz,[1,*] T. Kinoshita,[1] T. W. Hänsch,[1] and A. Hemmerich[2]
[1]*Sektion Physik, Ludwig-Maximilians-Universität, Schellingstraße 4, 80799 München, Germany and Max-Planck-Institüt für Quantenoptik, Hans-Kopfermannstraße 1, 85748 Garching bei München, Germany*
[2]*Institut für Laserphysik, Universität Hamburg, Jungiusstraße 9, 20355 Hamburg, Germany*
(Received 5 July 2000; published 4 June 2001)

We present the experimental realization of optical superlattices created by exposing laser cooled ^{85}Rb atoms to a bichromatic standing-wave light field. The two light frequencies are tuned close to the D_1 and D_2 lines of ^{85}Rb. The total optical potential seen by the atoms exhibits a modulation at the spatial beat period of the two light fields in addition to the typical periodicity on the scale of an optical wavelength. The bichromatic light field cools the atoms into the superlattice potential, resulting in a density modulation on a macroscopic scale. We have observed the density modulation directly in one- and three-dimensional superlattice configurations using an absorption imaging technique.

DOI: 10.1103/PhysRevA.64.011401 PACS number(s): 32.80.Pj, 42.50.Vk

In the last few years, optical lattices have been widely used as a model system for the study of fundamental concepts of quantum physics. The almost perfect symmetry of these arrays of light-bound atoms has made it possible to apply well-known techniques from condensed-matter physics such as Bragg diffraction [1] and to observe phenomena such as Bloch oscillations and Wannier-Stark ladders [2] that are hard to access in conventional crystals. The strong confinement of the atoms in harmonic potential wells has been exploited to study the dynamics of atomic wave packets [3] and to prepare atoms in well-defined quantum states of external degrees of freedom [4].

In optical lattices, atoms are trapped in micropotentials created by standing-wave light fields and thus the lattice spacing is generally on the order of several hundred nm. In most experiments to date only $\approx 1\%$ of the lattice sites were occupied; however, progress has recently been made in efficiently cooling dense samples in optical lattices [5] and achieving almost unity occupation of lattice sites [6]. This makes optical lattices a promising approach for achieving quantum degeneracy by all-optical means. Another prominent application under study is quantum computing in optical lattices [7]. A first experimental step in this direction was recently taken when quantum coherent dynamics in the double-well potentials of a far-off-resonant optical lattice was observed [8].

In this Rapid Communication, we report on the experimental observation of one- and three-dimensional bichromatic superlattices, created with a two-color light field, as proposed by Grimm *et al.* [9]. The depth of the micropotentials in these superlattices is modulated on a macroscopic scale, giving rise to preferential trapping of atoms at specific sites accompanied by a local density increase. If it becomes possible to trap individual atoms at well-defined superlattice sites, the macroscopic separation of superlattice wells could be used for addressing atoms and implementing quantum computing operations. Previously, one-dimensional (1D) superlattices have been demonstrated [10] and superlattice structures have been written with an atom-lithographic method [11], using monochromatic standing waves where some of the light beams subtended very small angles. A one-dimensional monochromatic lattice in which individual sites could be optically resolved has been realized using the long-wavelength light of a CO_2 laser [12].

By creating an optical lattice with two colors, the control over the lattice structure is greatly enhanced. In our bichromatic superlattices, two light fields are tuned to different atomic transitions, namely, the D_1 and D_2 lines of ^{85}Rb. This gives rise to a spatially modulated depth of the micropotentials where the atoms are expected to be preferentially trapped in the deepest micropotentials. Generally, preferential trapping of the atoms at certain locations can be attributed to the presence of a long-range component of the optical dipole force. This component, known as the rectified force [13], occurs in bichromatic light fields in addition to the usual component that alternates in sign on a wavelength scale. Rectified forces have been employed in a variety of experiments to deflect [14] and slow [15] atomic beams as well as to cool atoms [16]. In a bichromatic standing wave in the cascade configuration [17], trapping of atoms in macroscopic potential wells by means of rectified forces was achieved.

In our experiments the bichromatic optical lattice is loaded from a standard magneto-optical trap (MOT) with about 10^7 laser-cooled ^{85}Rb atoms in an atomic cloud of $\approx$1-mm diameter. The lattice light field is composed of a weak field at $\lambda_1 = 795$ nm, blue-detuned by $\approx 3\Gamma$ from the $5S_{1/2}$, $F_g = 3 \rightarrow 5P_{1/2}$, $F_{e1} = 2$ transition, and a strong field at $\lambda_2 = 780$ nm, tuned $\approx 300\Gamma$ below the $5S_{1/2}$, $F_g = 3 \rightarrow 5P_{3/2}$, $F_{e2} = 2,3,4$ transitions, where $\Gamma \approx 6$ MHz is the natural linewidth. The lattice laser beams have a diameter of 4 mm. A weak repumping laser recycles atoms that are pumped into the $F_g = 2$ hyperfine ground state. All laser frequencies are generated by grating-stabilized diode lasers, where the light for the off-resonance lattice field is amplified with a high-power tapered amplifier, since up to 100 mW are required to obtain sufficiently large light shifts.

*Present address: MIT, 26-255, 77 Massachusetts Ave., Cambridge, MA 02139.

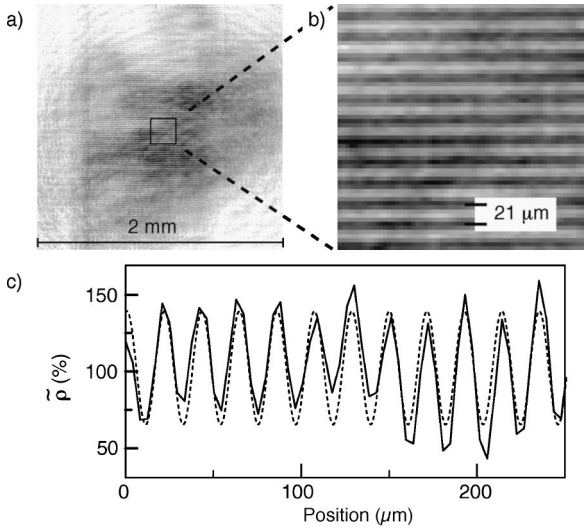

FIG. 1. (a) Typical absorption image of a bichromatic superlattice. (b) Magnified detail of (a). The image is normalized by taking the ratio of images with and without atoms. (c) Vertical cross section of (b). Plotted is the ratio of local density and average density as a function of the position. The dashed line is a sinusoidal fit, yielding a period of 21.3 μm$\pm$5%.

To create a one-dimensional bichromatic superlattice, we use a standing wave oriented along the vertical axis. The polarization geometry for both individual light fields is lin$\perp$lin, i.e., the standing wave is created by superimposing two counterpropagating beams with orthogonal linear polarization. Care is taken to spatially overlap the two light fields. Only zeroth order polarization optics are used in our setup, which ensures that the mismatch in polarization between the two colors is smaller than 2%. The spatial beat period for our choice of light fields is 21 μm as calculated using Eq. 1.

The atomic ensemble is typically exposed to the bichromatic light field for 5–10 ms. During this period a steady state of the vertical density distribution is reached, but the atomic cloud has not yet become diluted due to the lack of confinement in the horizontal dimensions. To detect the density modulation, we use an absorption imaging technique. After switching off the lattice light fields, the atomic ensemble is illuminated with a laser beam tuned close to the $5S_{1/2}$, $F_g=3\rightarrow 5P_{3/2}$, $F_e=4$ transition for a duration of 50 μs. The shadow cast by the atoms due to absorption of the probe light is magnified by a factor of 2 and imaged onto a CCD camera. The probe beam is aligned perpendicular to the lattice light field to better than 1°, since a larger deviation would diminish the contrast of the observed density modulation due to the finite size of the atomic cloud.

A typical absorption image of a 1D superlattice is depicted in Fig. 1. Figure 1(a) shows the whole atomic cloud where the gross structure reflects the density distribution of the MOT from which the superlattice is loaded. The magnified detail [Fig. 1(b)] of the absorption image clearly reveals that the atomic density distribution is spatially modulated. This density modulation could only be observed when we exposed the cloud of atoms to both standing-wave light fields simultaneously. While we have observed a density modulation over a wide range of light intensities, it is strongly dependent on the detunings, and in particular, their signs. Only if the D_1 light field is blue-detuned and the D_2 light field is red-detuned does the density modulation build up. In Fig. 1(c), we show a cross section of the density along the vertical direction in Fig. 1(b) where the density is obtained by taking the logarithm of the absorption signal. By fitting a sinusoidal function to the density modulation, we determine a spatial period of 21.3 μm$\pm$5%, which is in very good agreement with the expected value. A measurement of the density modulation decay after turning off the lattice fields allows us to roughly determine the temperature achieved with our bichromatic superlattice. It is on the order of 10 μK and thus in the same range as for monochromatic lattices.

From the amplitude of the density modulation in Fig. 1, we can deduce a factor of 1.5 for the increase of the maximum local density. However, this value has to be regarded as a conservative estimate, since imaging is limited by the diffraction-limited resolution of $\approx$6 μm, the pixel size of the camera of $\approx$8 μm, and the focal depth. The finite focal depth is presumably the main source of error, since the atomic ensemble extends over $\approx$1 mm along the probe beam, while the focal depth for imaging of a 10 μm sized object is only several hundred μm.

The principle of our bichromatic superlattice is best explained if we first consider the total light shift experienced by the atoms in the bichromatic light field. In addition to the usual periodicity on the scale of the optical wavelengths λ_1 and λ_2, the potential exhibits a spatial variation with a period given by

$$\Lambda_{sl}=\frac{1}{2}\frac{\lambda_1\lambda_2}{\lambda_1-\lambda_2}. \tag{1}$$

The explicit form of the optical potential in the limit of small optical excitation can be calculated by diagonalizing the total light-shift Hamiltonian [9,18], yielding the adiabatic ground-state potential curves. In Fig. 2(b) the adiabatic ground-state potentials for a ^{85}Rb atom interacting with a bichromatic standing-wave light field composed of blue-detuned D_1 light and red-detuned D_2 light are shown. As in the experiment, the polarization geometry is lin$\perp$lin (two counterpropagating laser beams with orthogonal linear polarizations) and the intensities of the two light fields are chosen such that the individual light shifts are of comparable magnitude. The fact that there are seven distinct adiabatic potential curves reflects the multiplicity of the $F_g=3$ hyperfine ground state.

From the shape of the adiabatic potentials alone, it is not evident at what places within a superlattice period the atoms are preferentially trapped. The location of these superlattice wells depends on the subtle interplay between the total optical potential and the spatially varying steady-state populations of the adiabatic states. These steady-state populations are determined by the local polarization of the D_1 light field that is responsible for optical pumping. Due to the rapid optical pumping, the average force on an atom is just given by the sum of the gradients of all micropotentials weighted by the populations. We illustrate this effect qualitatively in Fig. 2(c) by using a model in which the hyperfine structure is disregarded, i.e., an atom with a $J_g=1/2$ ground state and

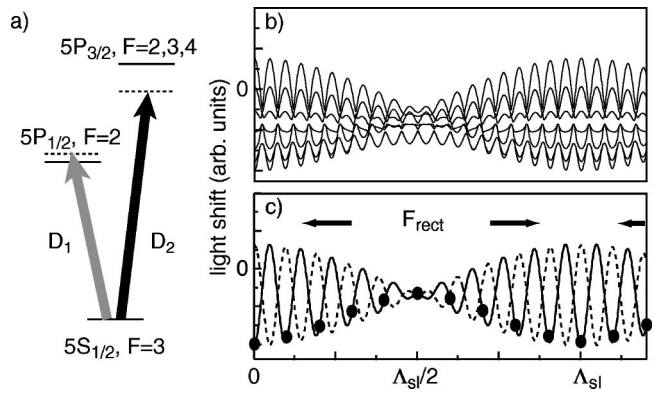

FIG. 2. (a) Level scheme of ^{85}Rb showing the levels relevant to the bichromatic light field. (b) Optical potentials for ^{85}Rb in the bichromatic standing wave with lin$\perp$lin polarization. To resolve the microscopic periodicity of the potential, the ratio λ_1/λ_2 has been artificially set to 11/10. (c) Optical potentials for a simplified case where the hyperfine structure is disregarded. The filled circles indicate the positions where the total population is found in the $m_g = +1/2$ sublevel (solid line). The arrows indicate the direction of the rectified force.

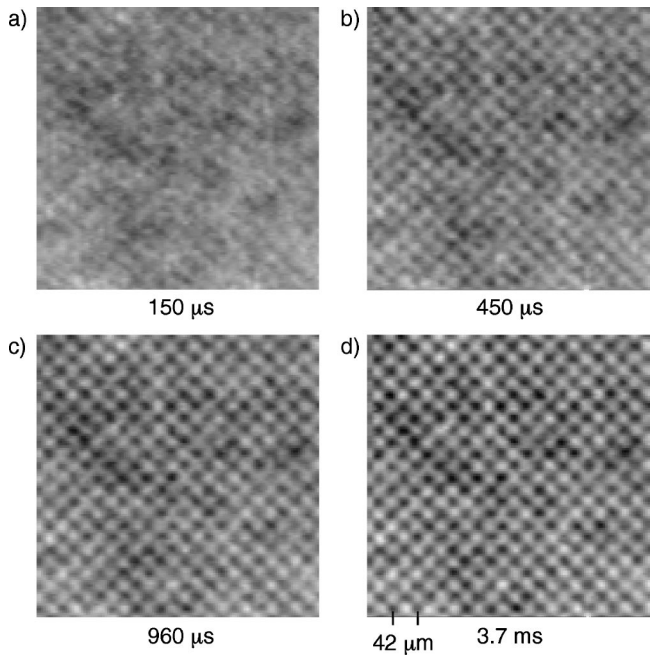

FIG. 3. Formation of the three-dimensional superlattice structure. The images are taken at various times after the bichromatic light field is turned on.

excited states with $J_{e1} = 1/2$ and $J_{e2} = 3/2$. We have indicated the positions at which the total population is found in the $m_g = +1/2$ sublevel. It can be seen that the atoms are preferentially pumped into this sublevel at locations where, due to the local gradient of the optical potential, they experience a force directed towards the deepest micropotentials. On a macroscopic scale, this gives rise to a long-range rectified force as indicated by the arrows in Fig. 2(b). The same reasoning for the direction of the rectified force applies if one considers the $m_g = -1/2$ magnetic sublevel. The cooling mechanism in the bichromatic potential is similar to the well-known polarization-gradient cooling mechanism [19] in a monochromatic light field. However, the long-range rectified force lends an additional directionality, which provides preferential cooling of the atoms into the deepest micropotentials. Since the atoms are almost decoupled from the D_1 light field at these positions and excitation due to the D_2 light field can be neglected to lowest order due to the large detuning, our bichromatic configuration can be seen as a purely optical gray or dark lattice [20]. In the original proposal of Grimm *et al.* [9], the light fields were chosen such that the atoms were preferentially cooled into the shallowest micropotentials. A general theoretical analysis of the cooling mechanisms in bichromatic standing waves can be found in [21].

It is straightforward to extend the bichromatic superlattice scheme to three dimensions. We use a setup with three pairwise orthogonal standing waves. The two horizontal standing waves are both linearly polarized in the horizontal plane, while the vertical one is circularly polarized. For the off-resonance D_2 light field, this yields a bcc lattice structure for appropriately adjusted time-phase differences between the standing waves [22]. This bcc structure should also be reflected in the periodicity of the 3D bichromatic superlattice. The edge length of the cubic superlattice unit cell is expected to be $2\Lambda_{sl} \approx 42\ \mu$m, since coincidences of the polarization patterns of the individual light fields are repeated with this periodicity.

To observe the 3D superlattice, we align the probe beam parallel to one axis of the lattice field and perpendicular to the other two. Thus, the bcc structure is projected onto a plane parallel to one of the surfaces of a unit cell and should yield a face-centered square structure in the absorption image. Typical absorption images of an atomic sample in a 3D bichromatic light field are shown in Fig. 3. The images in Fig. 3 are taken after different times of interaction between the lattice fields and the atoms. It is readily seen how the density modulation is building up, which is a clear indication for active cooling of the atoms into the superlattice wells. From Fig. 3(d), which is taken after a steady-state value of the density modulation is reached, we determine the period of the density modulation. We find 42.1 μm$\pm$5% for the horizontal direction and 42.5 μm$\pm$5% for the vertical direction. Analysis of the same image yields a peak density that is at least a factor of 2.5 larger than the average density. The same problems as in the 1D case prevent us from giving a more precise value for the enhancement of the local density. We plan to employ Bragg diffraction from superlattice planes to determine the density increase more accurately. The diffracted intensity will depend on localization in the superlattice wells, similar to previous work [3] where it depended on localization in the micropotentials. Another possibility to further analyze our bichromatic superlattices would be to look for self-induced Bragg-type light scattering [23].

Our choice of the 3D light-field geometry should in principle allow adiabatic transfer of the modulated density distribution from the bichromatic superlattice into an off-resonance monochromatic optical lattice. This would combine the locally enhanced filling factor of the superlattice with the simpler lattice geometry of a monochromatic lattice

and lower dissipation in the off-resonance light field. This might be useful for the realization of quantum-logic gates, since most of the proposed schemes [7] have considered monochromatic lattices but require that there be a probability that atoms are trapped at adjacent lattice sites. In preliminary experiments, we have seen that after adiabatically turning off only the D_1 light field, the density modulation decays more slowly by a factor of roughly 5 than in the case where both light fields are turned off simultaneously. We attribute this to an at least partial transfer of the atoms from the bichromatic lattice into a monochromatic D_2 lattice.

In conclusion, we have experimentally demonstrated that a well-designed bichromatic standing-wave light field can be used to create an optical superlattice in one as well as three dimensions. In contrast to previous observations of density modulations in a two-color MOT [24], our experimental findings are fully consistent with the model of a rectified force acting on the atoms in the bichromatic light field. In our scheme, the trapped atoms are almost decoupled from the lattice light fields and therefore density limitations due to light scattering by the atoms should be alleviated and, in principle, a density increase by more than the observed factor of 2.5 should be feasible.

T.K. acknowledges funding by the Alexander-von-Humboldt Stiftung.

[1] M. Weidemüller *et al.*, Phys. Rev. Lett. **75**, 4583 (1995); G. Birkl *et al.*, *ibid.* **75**, 2823 (1995).
[2] M. Ben Dahan *et al.*, Phys. Rev. Lett. **76**, 4508 (1996); S.R. Wilkinson *et al.*, *ibid.* **76**, 4512 (1996).
[3] A. Görlitz *et al.*, Phys. Rev. Lett. **78**, 2096 (1997); G. Raithel *et al.*, *ibid.* **78**, 2928 (1997); P. Rudy, R. Ejnisman, and N.P. Bigelow, *ibid.* **78**, 4906 (1997); M. Kozuma *et al.*, Phys. Rev. A **57**, R24 (1998).
[4] S.E. Hamann *et al.*, Phys. Rev. Lett. **80**, 4149 (1998); M. Morinaga *et al.*, *ibid.* **83**, 4037 (1999).
[5] A.J. Kerman *et al.*, Phys. Rev. Lett. **84**, 439 (2000).
[6] M.T. DePue *et al.*, Phys. Rev. Lett. **82**, 2262 (1999).
[7] G.K. Brennen *et al.*, Phys. Rev. Lett. **82**, 1060 (1999); D. Jaksch *et al.*, *ibid.* **82**, 1975 (1999); A. Hemmerich, Phys. Rev. A **60**, 943 (1999).
[8] D.L. Haycock *et al.*, Phys. Rev. Lett. **85**, 3365 (2000).
[9] R. Grimm, J. Söding, and Yu.B. Ovchinikov, Zh. Éksp. Teor. Fiz. **61**, 362 (1995) [JETP Lett. **61**, 367 (1995)].
[10] L. Guidoni and P. Verkerk, Phys. Rev. A **57**, R1501 (1998).
[11] T. Schulze *et al.*, Appl. Phys. B: Lasers Opt. **70**, 671 (2000).
[12] R. Scheunemann *et al.*, Phys. Rev. A **62**, 051801(R) (2000).
[13] A.P. Kazantsev and I.V. Krasnov, J. Opt. Soc. Am. B **6**, 2140 (1989).
[14] R. Grimm *et al.*, Phys. Rev. Lett. **65**, 1415 (1990); P.R. Hemmer *et al.*, *ibid.* **68**, 3148 (1992).
[15] J. Söding *et al.*, Phys. Rev. Lett. **78**, 1420 (1997).
[16] R. Gupta *et al.*, Phys. Rev. Lett. **71**, 3087 (1993).
[17] T.T. Grove *et al.*, Phys. Rev. A **51**, R4325 (1995).
[18] C. Cohen-Tannoudji, J. Dupont-Roc, and G. Grynberg, *Atom-photon Interactions: Basic Processes and Applications* (Wiley, New York, 1992).
[19] J. Dalibard and C. Cohen-Tannoudji, J. Opt. Soc. Am. B **6**, 2023 (1989).
[20] G. Grynberg and J.-Y. Courtois, Europhys. Lett. **27**, 41 (1994); A. Hemmerich *et al.*, Phys. Rev. Lett. **75**, 37 (1995).
[21] W. Alge *et al.*, Europhys. Lett. **39**, 491 (1997); Eur. Phys. J. D **6**, 133 (1999).
[22] A. Hemmerich and T.W. Hänsch, *Fundamentals of Quantum Optics III*, edited by F. Ehlotzky, Lecture Notes in Physics Vol. 420 (Springer Verlag, New York, 1993).
[23] P. Horak and H. Ritsch, Phys. Rev. A **55**, 2176 (1997).
[24] D.M.B.P. Milori *et al.*, Phys. Rev. A **59**, 3101 (1999).